JOURNAL OF MATERIALS SCIENCE 29 (1994) 164–168

Mechanical properties of (Y-TZP)-alumina–silicon carbide nanocomposites and the phase stability of Y-TZP particles in it

K. NIIHARA, N. ÜNAL*, A. NAKAHIRA
The Institute for Scientific and Industrial Research, Osaka University, Suita Campus, 8-1 Mihagaoka, Osaka, 567 Japan

Al_2O_3–SiC–ZrO_2 composites were investigated to obtain a better understanding of the effect of SiC particles and the stress-induced transformation of Y-TZP on its mechanical properties. The Al_2O_3–SiC–ZrO_2 composites were fabricated by hot pressing using γ-Al_2O_3, SiC and ZrO_2 mixtures. Fracture toughness and strength of Al_2O_3 were greatly improved by incorporating SiC and ZrO_2 particles which were located mainly inside and between Al_2O_3 grains, respectively. The toughening and strengthening mechanism of these composites and the phase stability of the tetragonal ZrO_2 in the composites before and after high-temperature annealing were investigated by scanning electron microscopy, transmission electron microscopy and X-ray diffraction. It was observed that there is a critical volume fraction of zirconia, above which the phase stability of the tetragonal zirconia increases, despite the grain growth of the zirconia. It is considered that another phenomenon, the residual stresses, affect the phase stability of the tetragonal zirconia. To remove the residual stresses the composites were annealed at 1100 °C. After slow cooling, the tetragonal zirconia became very unstable, especially in samples with the highest fabrication temperature and increasing zirconia content. Even quenching from 1100 °C caused an increase in the monoclinic phase of these samples.

1. Introduction

It is well known that the introduction of SiC or ZrO_2 particles or SiC whiskers into alumina ceramics enhances their mechanical properties [1–6]. Niihara *et al.* [7] incorporated SiC particles, on a submicrometre scale, in the Al_2O_3 matrix and observed significant improvements in the mechanical properties. The fracture mode of these composites was mainly transgranular. This may be attributed to the tensile hoop stresses around the SiC particles located in the matrix. The tensile hoop stresses are caused by the thermal expansion mismatch between the particle and the matrix. Niihara *et al.* produced Al_2O_3–SiC–ZrO_2 composites using 5% SiC and several amounts of partially stabilized zirconia to make use of tetragonal to monoclinic (t–m) phase transformation of zirconia as an additional toughening mechanism. In this way, they succeeded in increasing the fracture strength of the samples up to 1750 MPa and the fracture toughness up to about 6 $\mathrm{MPa\,m^{1/2}}$ [7]. In this study the dependence of the mechanical properties on the ZrO_2 content and on the fabrication temperature of the composites containing 10 vol % SiC particles was investigated. The t–m transformation was revealed using TEM and X-ray diffraction (XRD). In order to investigate the variation in the t–m transformation of the composites, they were annealed at 1100 °C. The phase stability of tetragonal zirconia before and after annealing was discussed.

2. Experimental procedure

γ-Al_2O_3 (grain size < 0.4 µm), β-SiC powder (< 0.3 µm) and 2,5Y-TZP powders (< 0.2 µm) were used to fabricate the composite materials. The compositions containing 10 vol % SiC and 10, 20 or 30 vol % ZrO_2 were milled 12 h in ethanol using high-purity Al_2O_3 balls. After drying, the mixture of powders was milled for 24 h without any liquid medium, and then hot pressed into the plates at 1500, 1600 or 1700 °C for 1 h and were cooled in the furnace. After cooling, the two parallel surfaces of the plates were ground using diamond discs, then they were cut into bars (width 3 mm). The bars were tested to determine *E*-modulus, Vickers hardness, fracture strength and fracture toughness. The densities of the fabricated composites were measured by Archimedes' method. The microstructures of the samples were investigated by means of SEM and TEM. The hardness and fracture toughness of the samples were measured by the indentation microfracture technique with the indentor load of 4.9–19.6 N.

---

* *Present address*: Akdeniz University. MYO, 7050-Antalya, Turkey.

0022-2461

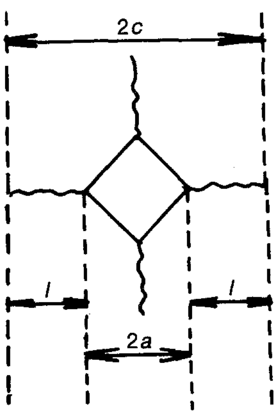

Figure 1 Vickers indentation damage and the crack lengths.

The K_{Ic} values were calculated using one of the following empirical equations [8].

For $c/a > 2.5$

$$(\Phi K_{Ic}/Ha^{1/2})\,(H/\Phi E)^{2/5} = 0.129\,(c/a)^{-3/2} \qquad (1)$$

For $0.25 < l/a < 2.5$

$$(\Phi K_{Ic}/Ha)\,(H/\Phi E)^{2/5} = 0.035\,(l/a)^{-1/2} \qquad (2)$$

where H is the Vickers hardness, E is the elastic modulus, Φ is the constriction factor. Φ was taken 3 in the calculations. Lengths c, l and a are shown in Fig. 1.

Fracture strength was determined using a three-point bending test over a 20 mm span. The tensile surfaces of the samples were polished by means of 1 μm diamond slurry. The edges of the tensile surfaces were bevelled in the same way. The crosshead speed of the bending machine was 0.5 mm min^{-1}.

The elastic moduli of the samples were determined by the resonance technique.

In order to determine the fracture mode, the fractured surfaces and the polished surfaces of the samples were investigated by SEM. The polished surfaces were etched in boiling phosphoric acid for 5 min to detect the grain boundaries. The average grain size of the samples was measured from scanning electron micrographs taken from the etched surfaces. X-ray diffraction analyses were performed to determine the peak heights of tetragonal and monoclinic zirconia and the following equations were utilized to calculate the volume fraction of the monoclinic phase [9].

$$V_m = \frac{PX_m}{1 + (P - 1)X_m} \qquad (3)$$

where X_m is the integrated intensity ratio and $P = 1.340$.

$$X_m = \frac{I_m(\bar{1}\,1\,1) + I_m(1\,1\,1)}{I_m(\bar{1}\,1\,1) + I_m(1\,1\,1) + I_t(1\,0\,1)} \qquad (4)$$

Subscripts m and t represent the monoclinic and the tetragonal phases, respectively. I_m and I_t are the peak heights of these phases. V_m is the volume fraction of the monoclinic phase and that of the tetragonal phase is $V_t = 1 - V_m$.

Calculation of V_m was also performed from the cut, ground and fractured surfaces.

To gain a better understanding of the effect of cutting, grinding or fracturing processes and the role of the internal stresses on the phase stability of zirconia particles, the samples were subjected to heat treatment. They were heated up to 1100 °C and were kept at this temperature for 1 h to transform the monoclinic zirconia grains obtained from cutting, grinding or fracturing back to the tetragonal phase. Because a temperature of 1650 °C or higher is necessary for ZrO_2 grain growth [10], 1100 °C is chosen as the annealing temperature to eliminate the grain growth. After annealing at 1100 °C some of the samples were quenched in air to obtain the high-temperature phases of zirconia at room temperature. The rest of the samples were cooled in the furnace to determine the effect of slow cooling.

3. Results and discussion

X-ray diffraction analysis indicated that the hot-pressed samples are composed of α-Al_2O_3, β-SiC, m-ZrO_2 and t-ZrO_2. SEM and TEM observations revealed that the SiC particles were mostly dispersed intragranular, in both Al_2O_3 and ZrO_2 grains (Figs 2 and 3). The ZrO_2 grains were mainly located on junctions of Al_2O_3 grains. The particle size of dispersed SiC was typically less than 0.1 μm, as shown in Fig. 3.

Using scanning electron micrographs it was revealed that the grain growth and agglomeration occurred on increasing the fabrication temperature from 1500 to 1700 °C.

The mechanical properties of the hot-pressed samples are seen in Figs 4–6 as a function of ZrO_2 volume fraction. The samples with 20 vol % ZrO_2 fabricated at 1600 and 1700 °C had the maximum fracture strength. At a fixed zirconia content, the fracture strength decreases as the temperature increases.

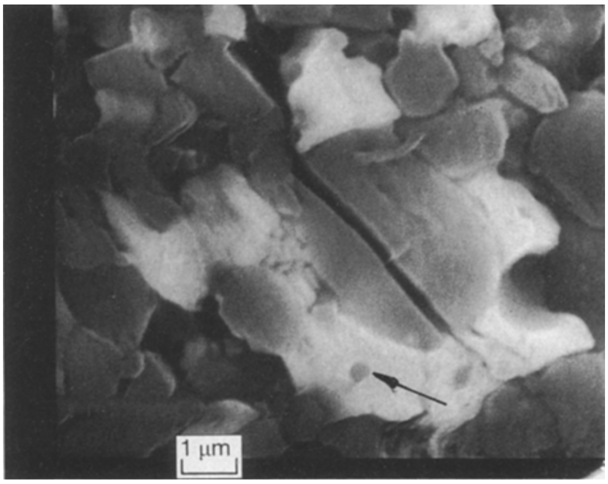

Figure 2 Scanning electron micrograph showing the location of SiC particles in the zirconia grains. White grains are zirconia. The arrow shows the SiC particle.

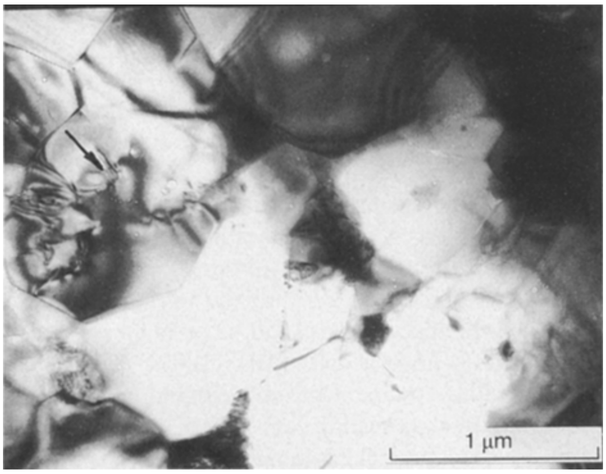

Figure 3 Transmission electron micrograph showing the location of SiC particles in an alumina grain. The white grains are alumina. The arrow shows the SiC particle.

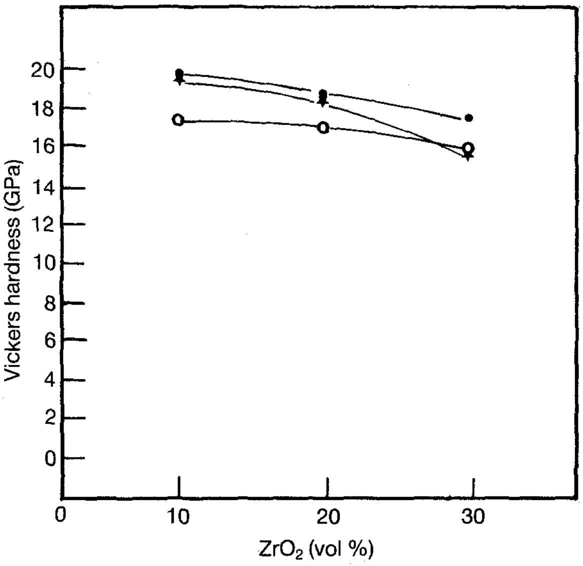

Figure 4 Variation of Vickers hardness with the volume fraction of ZrO_2 and temperature. (●) 1500 °C, (★) 1600 °C, (○) 1700 °C.

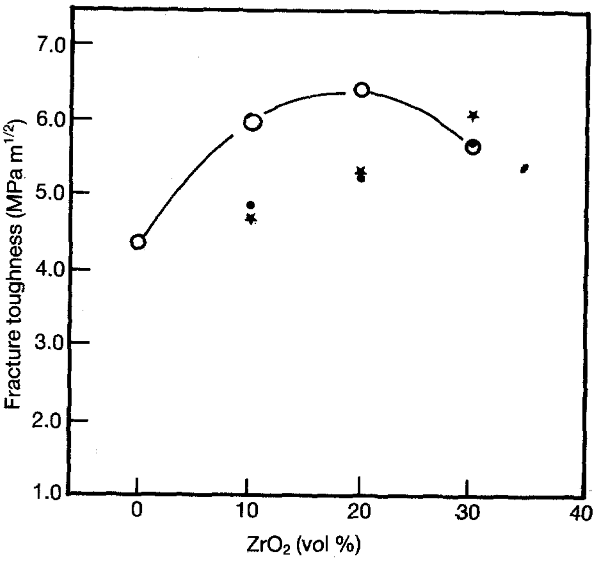

Figure 5 The change in fracture toughness with the volume fraction of zirconia at different sintering temperatures. (●) 1500 °C, (★) 1600 °C, (○) 1700 °C.

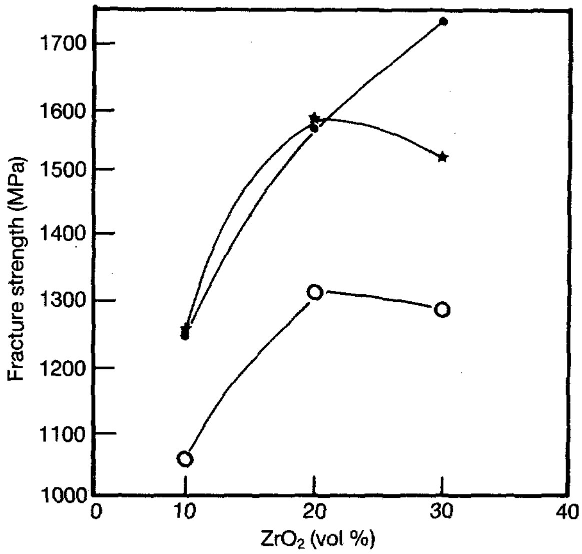

Figure 6 The change in fracture strength with the volume fraction of zirconia at different sintering temperatures. (●) 1500 °C, (★) 1600 °C, (○) 1700 °C.

TABLE I The average grain size of Al_2O_3 and ZrO_2 in the composites

Fab. temp. (°C)	ZrO_2 (vol %)	Alumina (μm)	Zirconia (μm)
1500	10	0.60	–
	20	0.62	0.51
	30	0.61	0.54
1600	10	0.75	0.56
	20	0.71	0.64
	30	0.74	0.66
1700	10	1.35	0.82
	20	1.47	1.37
	30	1.4	1.45

The average grain size of the samples is shown in Table I. It can be seen from Table I that the ZrO_2 content has almost no effect on the grain growth of Al_2O_3. It is well known that the increase in zirconia content inhibits the grain growth of Al_2O_3 [4]. An increase in temperature has more effect on the grain growth than an increase in the zirconia content of the composites. The average grain size of Al_2O_3 in the samples with 10 vol % ZrO_2 and 30 vol % ZrO_2 are close to each other at a fixed sintering temperature. These can be attributed to the greater agglomeration of ZrO_2 particles with higher ZrO_2 content.

Fig 7 shows the monoclinic zirconia content of the composites with various volume fractions of zirconia according to their fabrication temperature.

The monoclinic volume fractions of zirconia in the composites are listed in Table II, for the samples after fabrication, after annealing and quenching, after annealing and slow cooling.

It can be seen from Table II that the tetragonal phase are quite stable in the as-hot-pressed samples fabricated at 1500 and 1600 °C. The samples fabricated at 1700 °C showed higher rate of t–m transformation than those of the others. This may be caused by the grain growth of zirconia which pro-

TABLE II Volume fraction of monoclinic zirconia determined from the cut, ground and fractured surfaces of the samples

Fab. temp. (°C)	ZrO_2 (vol %)	As-hot-pressed			Heat treated				
					After quenching		After slow cooling		
		Cut	Ground	Fractured	Cut	Ground	Cut	Ground	Fractured
1500	10	9.7	8.6	5.1	5.08	10.76	11.81	11.81	12.85
	20	6.3	7.4	9.7	–	6.28	8.57	9.68	17.65
	30	1.3	5.1	4.5	0.0	6.28	–	–	11.81
1600	10	11.8	17.2	10.8	14.8	21.7	18.6	19.4	18.7
	20	9.6	15.8	15.8	12.8	25.8	31.3	48.7	49.8
	30	7.4	9.7	9.7	3.86	3.87	11.8	21.1	15.8
1700	10	57.1	59.0	47.0	50.7	60.25	63.6	71.8	64.0
	20	41.6	35.5	40.0	49.0	50.8	69.3	64.6	73.0
	30	12.9	8.5	24.0	16.73	17.65	63.8	42.0	59.2

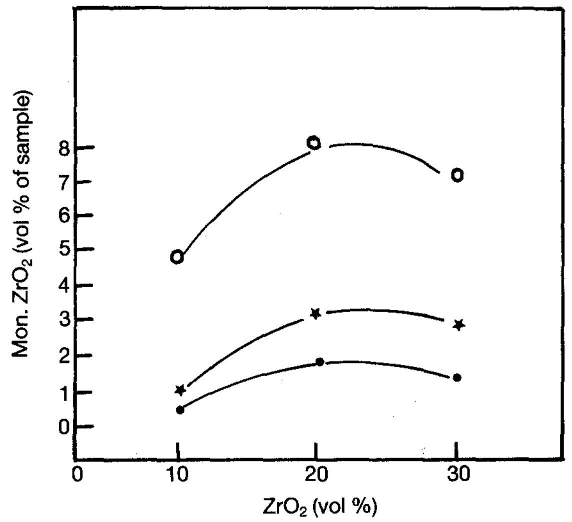

Figure 7 Relation between monoclinic ZrO_2 content of the fracture surfaces and the ZrO_2 content of the composites with variation in the fabrication temperature. (●) 1500 °C, (★) 1600 °C, (○) 1700 °C.

TABLE III Variation in the monoclinic fraction of the composites (fabricated at 1700 °C) with zirconia content after annealing and slow cooling

ZrO_2 in the composites (vol %)	M_1/M_2[a]		
	Cut surfaces	Ground surfaces	Fractured surfaces
10	1.11	1.21	1.36
20	1.66	1.82	1.82
30	4.94	6.46	2.46

[a] M_1, monoclinic fraction of zirconia, determined after annealing and slow cooling. M_2, monoclinic fraction of zirconia, determined after hot pressing.

motes the t–m transformation and/or the diminution of Y_2O_3 in the zirconia grains. On the other hand, despite the fact that samples with 10 vol % zirconia have a smaller grain size to those of 20 and 30 vol %, they have more monoclinic phase than those of 20 and 30 vol %. The t–m transformation in the samples with 30 vol % zirconia was suppressed. The same tendency was shown at the cut, ground and fractured surfaces. It was pointed out that in the zirconia-toughened alumina composites, tetragonal zirconia becomes less stable as the zirconia content increases [4]. In our case, it must be an another phenomenon which affects the phase stability of tetragonal zirconia despite the increased grain size. It is well known that the local residual stresses affect the phase stability of ZrO_2 [11]. Local residual stresses arise during cooling after the hot pressing of these composites. In the case of zirconia, the diffusion mechanism is ineffective below 1000 °C to eliminate internal stresses arising due to the thermal expansion mismatch of the phases in the matrix. Al_2O_3–ZrO_2–SiC nanocomposite is a multiphase system. There is a thermal expansion mismatch between alumina grains and SiC particles located in the alumina grains. There is also a thermal expansion mismatch between zirconia grains and SiC particles located in the zirconia grains; it also exists between alumina and zirconia grains.

To investigate the role of residual stresses, the composites were heat treated at 1100 °C and subjected to quenching in air or to slow cooling. The purpose of the quenching was to be able to compare the effect of slow cooling on the stability of the tetragonal phase. After quenching it is expected that the tetragonal phase would remain existent at room temperature. In our case, the amount of monoclinic phase generally increased even after quenching. The monoclinic–tetragonal phase transformation was observed only in a few composites, especially that fabricated at 1500 °C. All the composites showed enrichment of the monoclinic phase after annealing and subsequent slow cooling (Table II). This can be attributed to the stress relaxation of the samples during heat treatment. The rates of increase of the monoclinic fraction of zirconia are given in Table III for composites fabricated at 1700 °C. These rates are highest in the composites with 30 vol % zirconia. It could be concluded that the tetragonal zirconia grains which could not transform to monoclinic during cooling from fabrication temperature, could transform to monoclinic after removal of the residual stresses.

If the ZrO_2 content of the sample increases, grain growth occurs especially in the agglomerated grains. The SiC particles which were previously located in the grain boundaries, remain in the inside of the particles, and stress fields interact with each other. Therefore, these samples have more residual stresses than the

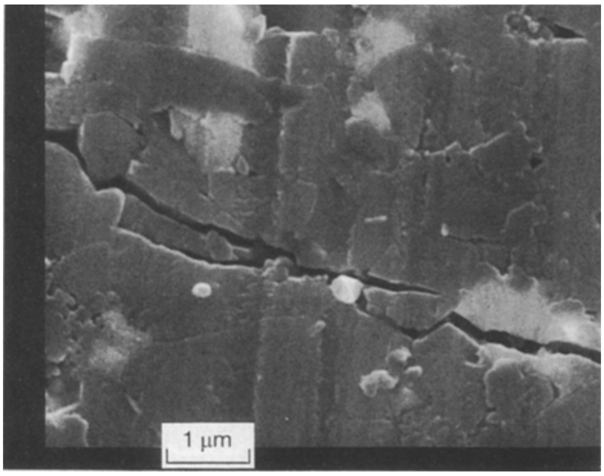

Figure 8 Scanning electron micrograph showing crack branching and crack propagation through the grains for the sample containing 10 vol % ZrO_2. Fabrication temperature = 1700 °C.

others and their zirconia grains may show less transformation to monoclinic during fracture after the fabrication. Claussen [12] reported that the tensile stresses in a matrix around spherical particles with radius R are given by (if $\alpha_m > \alpha_p$)

$$\sigma_t = \frac{(\alpha_m - \alpha_p)(T_1 - T_0)(R/r)^3}{2[1 + \nu_m)/2E_m + (1 - 2\nu_p)/E_p]} \tag{5}$$

where α_m, α_p, ν_m, ν_p, E_m, E_p are the thermal expansion coefficients, Poisson's ratios and Young's modulus of the matrix and the particles. T_1 is the temperature below which stresses no longer relax during cooling, T_0 is room temperature, r is the distance from the centre of the particle. As can be seen from Equation 5, the magnitude of tensile stresses depends exponentially on R/r.

SEM investigations showed that the fracture mode of the samples were mainly transgranular. The cracks passed mostly through the Al_2O_3 and ZrO_2 particles (Fig. 8). Internal stresses caused transgranular fracture. The crack tip was deflected around SiC particles in alumina and zirconia grains. Crack branching was found both in alumina and zirconia grains and this can contribute to toughening and strengthening of the composites.

4. Conclusions

1. Addition of some fine Y_2O_3-partially stabilized ZrO_2 in the Al_2O_3–SiC composites caused limited increase in stress-induced transformation toughness. However, the fracture strength of the composites was increased due to the location of extremely fine SiC particles in the zirconia grains. The SiC particles contributed to the strengthening of the composites by creating residual stresses which caused transgranular fracture. The cracks pass through the zirconia grains rather than the grain boundary.

2. The increase in the hot-pressing temperature causes the increase in the t–m transformation during loading at fixed zirconia content.

3. Although the composites with 30 vol % zirconia have larger zirconia grains, these composites showed less t–m transformation than those with 10 and 20 vol % zirconia during loading. This may be the result of the increased residual stresses due to the thermal expansion mismatch between the SiC particles and the zirconia grains. On the other hand, it could be recognized from scanning electron micrographs that in the samples with 30 vol % zirconia, some Al_2O_3 grains remained inside the ZrO_2 particles. In this case, additional tensile stresses can arise in the ZrO_2 grains around the Al_2O_3 particles.

4. After heating the composites up to 1100 °C and quenching, it could be expected that some of the monoclinic zirconia particles would have transformed back to the tetragonal form. It was observed that the composites (cut, ground and fractured surfaces) generally showed more monoclinic phase after than before quenching. The monoclinic volume fraction of zirconia increased even more after annealing and subsequent slow cooling. This can be attributed to the removal of the residual stresses during the high-temperature annealing. The samples with higher ZrO_2 contents showed more transformation to monoclinic after heat treatment. It can be concluded that the ZrO_2 particles with higher residual stresses can transform to monoclinic easily after removal of the residual stresses.

5. A high amount of microcracking was obtained after annealing of the samples which were produced at 1600 and 1700 °C. This makes these composites unsuitable for high-temperature applications. In terms of the fracture strength, fracture toughness and the phase stability at higher temperatures, the best result is obtained in the composites produced at 1500 °C. It can be concluded that there is a critical volume fraction and grain size which benefits from the addition of Y-TZP in the alumina–silicon carbide composites.

References

1. J. WANG and R. STEWENS, *J. Mater. Sci.* **24** (1989) 3421.
2. D. J. GREEN, *J. Am. Ceram. Soc.* **65** (1982) 610.
3. K. NIIHARA and A. NAKAHIRA, in "The Proceedings of the 7th CIMTEC-World Ceramic Congress", Montecatini Terme, Pistoria, Italy, 24–30 June 1990. edited by P. Vincentini.
4. Q. L. GE, T. C. LEI and Y. ZHOU, *Mater. Sci. Technol.* **7** (1991) 490.
5. M. RÜHLE, N. CLAUSSEN and A. H. HEUER, *J. Am. Ceram. Soc.* **69** (1986) 195.
6. P. F. BECHER, *ibid.* **74** (1991) 255.
7. A. NAKAHIRA, Y. FUKUSHIMA and K. NIIHARA, private communications (December, 1990).
8. K. NIIHARA, R. MORENA and D. P. H. HASSELMAN, *J. Mater. Sci. Lett.* **1** (1982) 13.
9. H. TORAYA, M. YOSHIMURA and S. SOMIYA, *J. Am. Ceram. Soc.* **6** (1984) C-119.
10. K. R. WILFINGER and W. R. CANNON, *ibid.* **72** (1989) 1256.
11. M. HIRANO and H. INADA, *ibid.* **74** (1991) 606.
12. N. CLAUSSEN, *ibid.* **59** (1976) 49.

Received 6 October 1992
and accepted 11 March 1993